International Journal of Thermal Sciences 48 (2009) 1607–1618

Contents lists available at ScienceDirect

International Journal of Thermal Sciences

www.elsevier.com/locate/ijts

Influence of channel geometry on the performance of a counter flow microchannel heat exchanger

Mushtaq I. Hasan [a,1], A.A. Rageb [a,2], M. Yaghoubi [b,*], Homayon Homayoni [c,3]

[a] Mechanical Engineering Department, College of Engineering, Thi-Qar University, Iraq
[b] Academy of Sciences – Iran, Shiraz University, Zand Street, Shiraz 71348-51154, Iran
[c] Department of Mechanical Engineering, Shiraz University, Zand Street, Shiraz 71348-51154, Iran

ARTICLE INFO

Article history:
Received 11 September 2008
Received in revised form 25 December 2008
Accepted 5 January 2009
Available online 7 February 2009

Keywords:
Microchannel size
Heat transfer
Channel shape
Thermal performance
Thermal effectiveness
Numerical simulation

ABSTRACT

Microchannel heat exchangers (MCHE) can be made with channels of various geometries. Their size and shape may have considerable effect on the thermal and hydraulic performance of a heat exchanger. In this paper numerical simulation is carried out to solve 3D developing flow and 3D conjugate heat transfer of a balanced counter flow microchannel heat exchanger (CFMCHE) to evaluate the effect of size and shape of channels on the performance of CFMCHE for the same volume of heat exchanger. The effect of shape of the channels on its performance is studied for different channel cross-sections such as circular, square, rectangular, iso-triangular and trapezoidal. Results show that for the same volume of a heat exchanger, increasing the number of channels lead to increase in both effectiveness and pressure drop. Moreover circular channels give the best overall performance (thermal and hydraulic) among various channel shapes. New correlations are developed to predict the value of heat exchanger effectiveness and performance index as a function of relative size of channels with overall heat exchanger volume, Reynolds number and thermal conductivity ratio.

1. Introduction

In recent years, progress in micro fabrication and assembling various small systems has lead to the development of extremely small scale machines commonly referred to as MEMS (Micro Electromechanical Systems). These systems are generally defined as electro mechanical devices having a characteristic length scale between 1 mm and 1 μm such as microchannel heat exchangers, microreactors, micro sensors, etc. [1]. Microchannel heat exchangers have found applications in highly specialized areas such as microelectronics cooling, aerospace, biomedical processes, metrology, robotics, telecommunications and automotive industries [1,2]. Channel size and cross sectional shape can have significant influence on the fluid flow and heat transfer characteristics in such microchannels.

Conventional design techniques for conventional heat exchangers such as F correction charts or ε–NTU relations cannot be applied directly to the microchannel heat exchangers since for their design it is assumed a constant value of overall heat transfer coefficient U. The value of heat transfer coefficients can be obtained using various correlations for individual ducts. While in counter flow microchannel heat exchangers (CFMCHE), the area of the walls separating the channels are comparable to the area of the channels and thermally fully developed flow may not exist over a large portion of the heat exchanger. For such condition, heat conduction in thick walls, short length of heat exchanger with developing flow, and the entrance region will play an important role. Due to these two important parameters (entrance region and axial conduction in the walls) are variables along the CFMCHE, and specific simulation must be made to calculate temperature distribution and then calculating local value of U in each point along the heat exchanger for its thermal design consideration.

The cooling concept of microchannel heat sinks was first introduced by Tuckerman and Pease [3], and ever since, the heat transfer and fluid flow characteristics in microchannels and microchannel heat sinks have been studied extensively. Peng and Peterson [4] performed experimental investigations on pressure drop and convective heat transfer of water flowing in rectangular microchannels and found that the cross-sectional aspect ratio had significant influence on the pressure drop and convective heat transfer in both laminar and turbulent flows.

Rachkovskij et al. [5] studied heat transfer in micro tubes of cross flow micro heat exchanger and examined the changes in heat transfer due to decrease of tube size and relative length. An esti-

* Corresponding author. Tel.: +98 9171184335; fax: +98 711 230 16 72.
E-mail addresses: mushtaq76h@yahoo.com (M.I. Hasan), muhsinrageb@yahoo.ie (A.A. Rageb), yaghoub@shirazu.ac.ir (M. Yaghoubi), homayonih@shirazu.ac.ir (H. Homayoni).
[1] Tel.: +9647801140094.
[2] Tel.: +9647801475072.
[3] Tel.: +98 9138688718; fax: +98 711 230 16 72.

1290-0729/$ – see front matter
doi:10.1016/j.ijthermalsci.2009.01.004

Nomenclature

A	cross-sectional area ..... m^2	z	horizontal coordinate ..... m
a, b	sides of trapezoidal and triangular channels ..... m	ΔP	pressure drop across heat exchanger ..... Pa
C_p	specific heat ..... J/(kg K)		
D_h	hydraulic diameter ..... m	*Greek symbols*	
H	channel height ..... m	η	performance index ..... m^2/N
h	convection heat transfer coefficient ..... $W/m^2 K$	η^*	performance factor
k	thermal conductivity ..... W/m K	ε	heat exchanger effectiveness
L	channel length ..... m	μ	dynamic viscosity ..... Pa/s
LMTD	long mean temperature difference	ρ	density ..... kg/m^3
m	mass flow rate ..... kg/s		
NTU	number of transfer units	*Dimensionless groups*	
P	pressure ..... Pa	$Kr = k_s/k_f$	thermal conductivity ratio
q	heat transfer rate ..... W	$Re = \frac{\rho u_i D_h}{\mu}$	Reynolds number
q_{max}	maximum heat transfer rate ..... W	*Vr*	void ratio; $Vr =$ Volume of single channel to the volume of overall heat exchanger
T	temperature ..... K		
t	separating wall thickness ..... m	*Subscripts*	
u	fluid x-component velocity ..... m/s	c	cold fluid
U	overall heat transfer coefficient ..... $W/m^2 K$	f	fluid
UA	thermal conductance ..... W/K	h	hot fluid
v	fluid y-component velocity ..... m/s	i	inlet
V	volumetric flow rate ..... m^3/s	max	maximum value
v_{in}	average velocity ..... m/s	min	minimum value
w	fluid z-component velocity ..... m/s	o	outlet
W_{ch}	channel width ..... m	s	solid
x	axial coordinate ..... m	w	wall
y	vertical coordinate ..... m		

mated, volumetric heat transfer coefficient of a single symmetric air–air micro cross flow heat exchanger modules of 50 mm^3 volume and 6 mm height is 4.3 $MW/m^3 K$ (at 260 Pa pressure drop, temperature difference of 5 K, micro tube size of 128×1200 μm). The increase in temperature of axial conduction under conditions of decreasing relative tube length leads to a decrease of heat exchange in micro tube. However, this effect should be taken into account for very short pipes with diameters of the order of their length. Also they found that the influence of the hydrodynamically entrance region does not change with a decrease in relative length of micro tube.

Albakhit et al. [6] numerically investigated the flow and heat transfer in parallel flow microchannel heat exchangers. They used a hybrid approach, in which the nonlinear momentum equations for one or two channels were solved using CFD codes. The velocity field was an input into a user developed code for solving the energy equation and they studied heat transfer for thermally developing laminar flow in two parallel rectangular channels which represent some kind of heat exchangers. From the results, it is found that in the entrance region the developing velocity profiles lead to higher values of overall heat transfer coefficient.

Brandner et al. [7] studied various microstructured cross flow heat exchangers and compared their thermal performances. They found that heat transfer in micro heat exchanger can be enhanced by decreasing the hydraulic diameter of microchannels. They even fabricated heat exchangers with two different layouts of micro column arrays (aligned and staggered) and compared these devices with respect to their heat transfer capabilities at a given mass flow. The staggered array of microcolumns maximized heat transfer in a given active volume and at the same time it was favorable regarding cocurrent minimization of pressure drop across the heat exchanger.

Foli et al. [8] presented two methods for determining the optimal design parameters of microchannels in microchannel heat exchanger (MCHE) for maximizing heat transfer rate subjected to specified design constraints. The first approach that combines CFD with the analytical solution of simplified transport equations for momentum and heat transfer is used to optimize the dimensions of a microchannel with predetermined geometry. It is used to find the optimum value of aspect ratio of channels. The second approach involves the usage of multi-objective genetic algorithms in combination with CFD. It has been demonstrated that performance of a MCHE depends on the operating conditions and aspect ratio of the microchannels that make up the flow passages.

Ngo et al. [9] investigated numerically the thermal hydraulic characteristics of a new microchannel heat exchangers with *s*-shaped and zigzag fins using 3D fluid dynamic (3D CFD) FLUENT code. They fund that the microchannels heat exchanger (MCHE) with *s*-shaped fins provided 6–7 times lower pressure drop while maintaining heat transfer performance that was almost equivalent to that of a conventional MCHE with zigzag fins. Correlations of Nusselt number and pressure drop factors for new MCHE with *s*-shaped fins and for a zigzag fins as a function of Reynolds number and Prandtl number were developed.

Literature shows that the microchannels and microchannels heat sinks were studied extensively but there are limited researches related to the performance of two fluids microchannel heat exchangers and there are no comprehensive investigations to study the effect of channels shape on the performance of two fluids CFMCHE. Thus the objective of this study is to investigate the effect of size of channels and various shapes on the overall thermal and hydraulic performance of balanced counter flow microchannel heat exchangers.

2. Mathematical model

Schematic structure of a counter flow microchannel heat exchanger with square channels is shown in Fig. 1. Fig. 2 illustrates details of channels with square/rectangular, circular, trapezoidal and iso-triangular profiles.

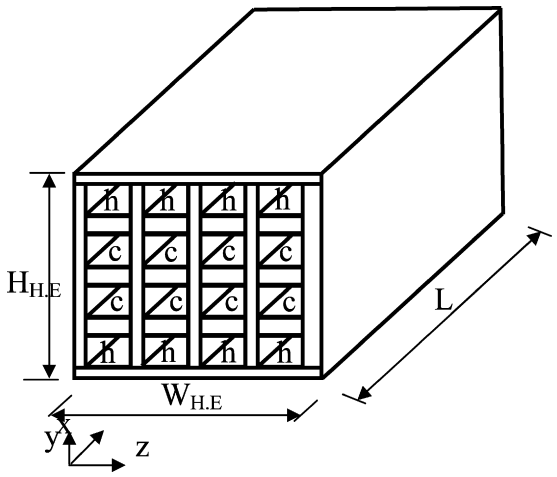

Fig. 1. A schematic model of a CFMCHE.

To study the entire CFMCHE numerically, it is complicated and needs huge CPU time. Due to symmetry between channels rows we will consider an individual heat exchange unite which consists of two channels (hot and cold) and a separating wall as shown in Fig. 2. If a CFMCHE has 16 channels in total (8 channels for each of the fluids) then the number of heat exchange unit would be 8. The volume of each heat exchange unit is determined by dividing the volume of the CFMCHE by the total number of heat exchange units with fixed value of wall thickness. Heat is transferred from hot fluid to cold fluid through the thick wall separating them and this heat exchange unite represents a complete CFMCHE and gives an adequate indication about its performance.

Assumptions:

(1) The CFMCHE operates under steady state conditions.
(2) The fluids do not undergo phase change while moving through the CFMCHE.
(3) The ends of the wall separating the channels are insulated.
(4) No slip boundary condition is assumed in the channels.
(5) Viscous dissipation, flow maldistribution and external heat transfer in the CFMCHE are neglected.
(6) Thermophysical properties of the fluids and heat exchanger material are assumed to be constants.

The governing equations and its boundary conditions in Cartesian coordinates for 3D, laminar incompressible flow (square and rectangular shapes) are:

Continuity equation

$$\frac{\partial u_j}{\partial x}+\frac{\partial v_j}{\partial y}+\frac{\partial w_j}{\partial z}=0 \tag{1}$$

Momentum equations

$$u_j\frac{\partial u_j}{\partial x}+v_j\frac{\partial u_j}{\partial y}+w_j\frac{\partial u_j}{\partial z} =-\frac{1}{\rho_j}\frac{\partial P}{\partial x}+\frac{\mu_j}{\rho_j}\left(\frac{\partial^2 u_j}{\partial x^2}+\frac{\partial^2 u_j}{\partial y^2}+\frac{\partial^2 u_j}{\partial z^2}\right) \tag{2}$$

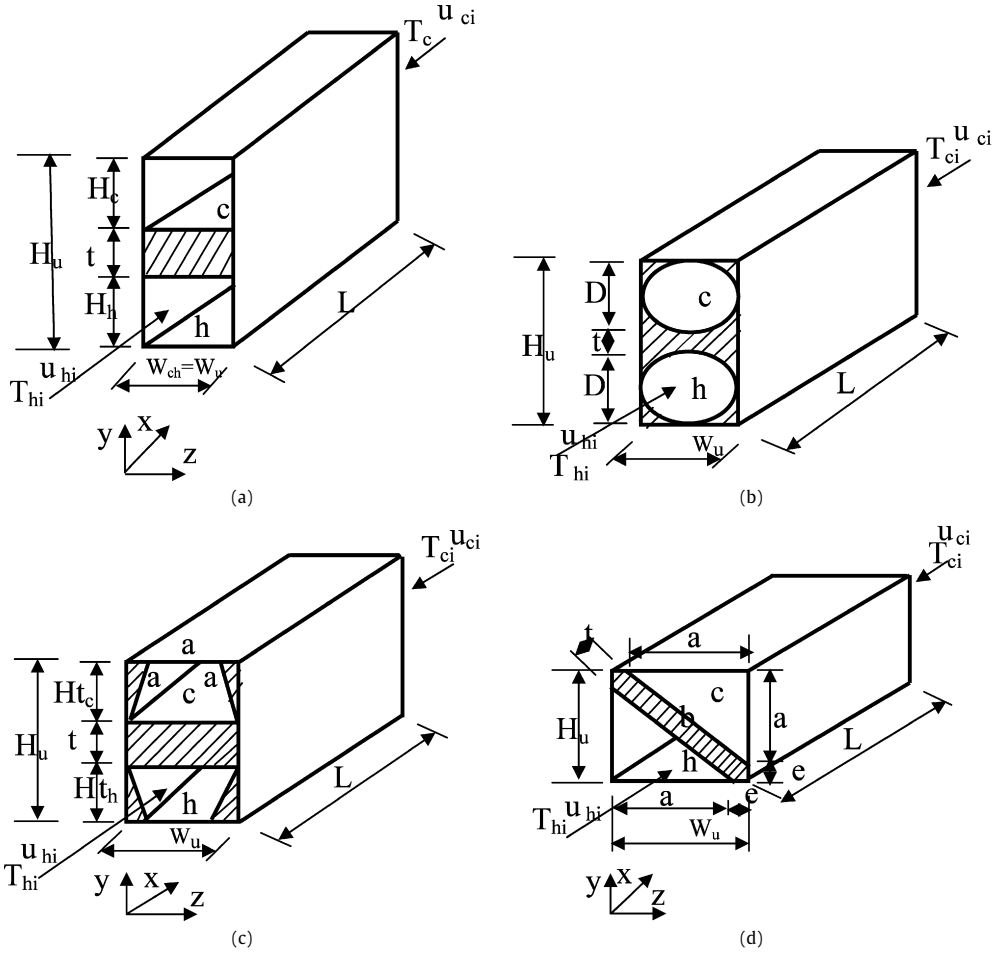

Fig. 2. A schematic of a heat exchange unite with (a) square and rectangular channels, (b) circular channels, (c) trapezoidal channels, (d) triangular channels.

$$u_j\frac{\partial v_j}{\partial x}+v_j\frac{\partial v_j}{\partial y}+w_j\frac{\partial v_j}{\partial z}$$
$$=-\frac{1}{\rho_j}\frac{\partial P}{\partial y}+\frac{\mu_j}{\rho_j}\left(\frac{\partial^2 v_j}{\partial x^2}+\frac{\partial^2 v_j}{\partial y^2}+\frac{\partial^2 v_j}{\partial z^2}\right) \quad (3)$$

$$u_j\frac{\partial w_j}{\partial x}+v_j\frac{\partial w_j}{\partial y}+w_j\frac{\partial w_j}{\partial z}$$
$$=-\frac{1}{\rho_j}\frac{\partial P}{\partial z}+\frac{\mu_j}{\rho_j}\left(\frac{\partial^2 w_j}{\partial x^2}+\frac{\partial^2 w_j}{\partial y^2}+\frac{\partial^2 w_j}{\partial z^2}\right) \quad (4)$$

Energy equation

$$u_j\frac{\partial T_j}{\partial x}+v_j\frac{\partial T_j}{\partial y}+w_j\frac{\partial T_j}{\partial z}$$
$$=\frac{k_j}{\rho_j Cp_j}\left(\frac{\partial^2 T_j}{\partial x^2}+\frac{\partial^2 T_j}{\partial y^2}+\frac{\partial^2 T_j}{\partial z^2}\right) \quad (5)$$

Where $j=h$ and c for hot and cold channels, respectively.

The energy equation for the solid wall is

$$\frac{\partial^2 T_s}{\partial x^2}+\frac{\partial^2 T_s}{\partial y^2}+\frac{\partial^2 T_s}{\partial z^2}=0 \quad (6)$$

The boundary conditions are:

Lower channel (hot fluid) $(0<y<H_h)$

at $x=0$

$$u_h=u_{hi},\qquad v_h=w_h=0,\qquad T_h=T_{hi}$$

at $x=L$

$$\frac{\partial u_h}{\partial x}=v_h=w_h=0,\qquad \frac{\partial T_h}{\partial x}=0$$

at $z=0$

$$u_h=v_h=w_h=0,\qquad \frac{\partial T_h}{\partial z}=0$$

at $z=W_{ch}$

$$u_h=v_h=w_h=0,\qquad \frac{\partial T_h}{\partial z}=0$$

at $y=0$

$$u_h=v_h=w_h=0,\qquad \frac{\partial T_h}{\partial y}=0$$

Solid–fluid interface

at $y=H_h$

$$u_h=v_h=w_h=0,\qquad -k_h\frac{\partial T_h}{\partial y}=-k_s\frac{\partial T_s}{\partial y}$$

Upper channel (cold fluid) $(H_h+t<y<H_h+t+H_c)$:

at $x=0$

$$\frac{\partial u_c}{\partial x}=v_c=w_c=0,\qquad \frac{\partial T_c}{\partial x}=0$$

at $x=L$

$$u_c=u_{ci},\qquad v_c=w_c=0,\qquad T_c=T_{ci}$$

at $z=0$

$$u_c=v_c=w_c=0,\qquad \frac{\partial T_c}{\partial z}=0$$

at $z=W_{ch}$

$$u_c=v_c=w_c=0,\qquad \frac{\partial T_c}{\partial z}=0$$

at $y=(H_h+t+H_c)$

$$u_c=v_c=w_c=0,\qquad \frac{\partial T_c}{\partial y}=0$$

Solid–fluid interface

at $y=(H_h+t)$

$$u_c=v_c=w_c=0,\qquad -k_c\frac{\partial T_c}{\partial y}=-k_s\frac{\partial T_s}{\partial y}$$

Solid wall B.C. $(H_h<y<H_h+t)$:

at $x=0,\ L$

$$\frac{\partial T_s}{\partial x}=0$$

at $z=0,\ W_{ch}$

$$\frac{\partial T_s}{\partial z}=0$$

at $y=H_h$

$$-k_h\frac{\partial T_h}{\partial y}=-k_s\frac{\partial T_s}{\partial y}$$

at $y=H_h+t$

$$-k_c\frac{\partial T_c}{\partial y}=-k_s\frac{\partial T_s}{\partial y}$$

For circular shape governing equations and B.C. in cylindrical coordinates were used. Also for trapezoidal and iso-triangular shapes a transformation of coordinates is used from physical space into computational space [10].

By solving the above governing equations using FLUENT 6.3 code the velocity distribution, pressure and temperature distribution are determined in the fluid and solid domains. From these distributions one can determine heat exchanger effectiveness, thermal conductance, heat transfer rate, pressure drop, pumping power required, overall heat transfer coefficient and overall performance index.

Heat exchanger effectiveness is the ratio of actual heat transfer to the maximum possible heat that can be transferred:

$$\varepsilon=\frac{q}{q_{max}} \quad (7)$$

where

$$q_{max}=C_{min}(T_{hi}-T_{ci}) \quad (8)$$

and

$$q=C_h(T_{hi}-T_{ho})=C_c(T_{co}-T_{ci}) \quad (9)$$

where

$C_h=mC_{p_h}$ and $C_c=mC_{p_c}$

Thermal conductance

$$UA=\frac{q}{LMTD} \quad (10)$$

$$LMTD=\frac{(T_{ho}-T_{ci})-(T_{hi}-T_{co})}{Ln\frac{T_{ho}-T_{ci}}{T_{hi}-T_{co}}} \quad (11)$$

So

$$\varepsilon=\frac{C_h(T_{hi}-T_{ho})}{C_{min}(T_{hi}-T_{ci})}=\frac{C_c(T_{co}-T_{ci})}{C_{min}(T_{hi}-T_{ci})} \quad (12)$$

The pumping power required to circulate hot and cold fluids in a CFMCHE is:

$$P.P=V_h\Delta P_h+V_c\Delta P_c \quad (13)$$

Where V is the volumetric flow rate (m^3/s).

$$V = v_{\text{in}} A \tag{14}$$

$$\Delta P_t = \Delta P_h + \Delta P_c = (P_{hi} - P_{ho}) + (P_{ci} - P_{co}) \tag{15}$$

Where ΔP_t is total pressure drop in heat exchange unit.

To calculate the overall performance of a counter flow MCHE, performance index is determined, which is represented by the ratio of CFMCHE effectiveness to the total pressure drop [11]. Performance index link the thermal and hydrodynamic performance to obtain an indication about the overall exchanger performance.

$$\eta = \frac{\varepsilon}{\Delta P_t} \tag{16}$$

A different form of performance index defined as the ratio of heat transferred between the fluids to total pumping power which can be used for determining overall performance of a CFMCHE as:

$$\eta^* = \frac{q}{P.P} \tag{17}$$

Both η and η^* can be used to obtain practical and physical indication about the exchangers overall performance. They link the thermal and hydrodynamic performances of the exchanger and the trends of variation of η and η^* are the same although their values are different.

3. Numerical solution

A computational fluid dynamic code is used to calculate flow velocity, pressure and temperature in the channels of a CFMCHE. Finite volume method (FVM) was used to convert the governing equations to algebraic equations accomplished using an "upwind" scheme. The SIMPLE algorithm was used to enforce mass conservation and to obtain pressure field [12]. The segregated solver was used to solve the governing integral equations for the conservation of mass, momentum and energy.

A mesh was generated by descretizing the computational domain (two channels and the separating wall). For a square channel of length $L = 10$ mm, channel height $H = 100$ μm, width $W = 100$ μm and wall thickness $t = 50$ μm, the mesh used is hexahedral elements. For a flow of $Re = 50$ three mesh sizes were used. The first mesh set was $(90 \times 16 \times 16)$ and $(90 \times 8 \times 16)$ in x-, y-, and z-directions for channels and wall respectively. The second mesh was $(110 \times 20 \times 20)$, and $(110 \times 10 \times 20)$ and the third mesh was $(110 \times 25 \times 25)$ and $(110 \times 15 \times 25)$. The computational results for CFMCHE effectiveness and central velocity in the fully developed region for the three meshes are listed in Table 1.

Table 1 shows that the solution becomes almost independent of grid size and from second configuration further increase the grids will not have a significant effect on the solution and results of such arrangement are acceptable.

The grid size of $(110 \times 25 \times 25)$, $(110 \times 15 \times 25)$ was used for the square shape. The dimensions of shapes other than the square were calculated based on fixed value of heat exchange unit volume of $(2.5 \times 10^{-10}\ \text{m}^3)$. For the rectangular channels with aspect ratio of 0.5 the channel width $W_{\text{ch}} = 135$ μm, channel height $H = 67.5$ μm, length $L = 10$ mm and wall thickness $t = 50$ μm. For circular channels the diameter $D = 100$ μm, length $L = 10$ mm and wall thickness $t = 50$ μm. For the trapezoidal channels the channel width $W_{\text{ch}} = 143.5$ μm, channel sides $a = 71.75$ μm, channel height $H = 62.1$ μm, length $L = 10$ mm and wall thickness $t = 50$ μm. For triangular channels the channel sides $a = 122.7$ μm, channel long side $b = 173.5$ μm, length $L = 10$ mm and wall thickness $t = 50$ μm. The grid size used for (rectangular, circular, trapezoidal and triangular) shapes are the same for square in the x-direction while in y- and z-directions. The interval size of grid was calculated by dividing the dimensions of square channel by the number of points in the grid used and the interval size was used to mesh the channels. The convergence rate to control the solution for momentum and energy equations were set to be less than 10^{-6}.

Table 1
Grid independent study.

Mesh configuration	Effectiveness	Fully developed central velocity
1	0.4281	0.6401 m/s
2	0.4226	0.6489 m/s
3	0.4222	0.6490 m/s

4. Results and discussion

For thermal analysis the fluid used is water with constant properties determined at the mean temperature across the entire length of channels. The inlet temperatures of hot and cold fluids used as boundary conditions are $T_{hi} = 373$ K and $T_{ci} = 293$ K. The inlet velocities are computed according to the value of Reynolds number, hydraulic diameter and the properties of fluid. Reynolds number is

$$Re = \frac{\rho u_i D_h}{\mu} \tag{18}$$

where

$$D_h = \frac{2(H_{\text{ch}} W_{\text{ch}})}{H_{\text{ch}} + W_{\text{ch}}} \tag{19}$$

The thermal conductivity ratio used in our calculations is the ratio of thermal conductivity of solid wall to the thermal conductivity of fluid, $Kr = k_s/k_f$. Transition from laminar to turbulent flow in microchannels is occur early compared with the flow in conventional channels. The value of $Re = 1000$ is nearly agreed as the transition value at which the flow changes from laminar to turbulent in microchannels [13–16]. In this paper the value of Reynolds number is always selected below 1000 and maximum value of Re is chosen 900 to ensure that the flow is in the laminar region.

To check the validity of built numerical model, verification was made by solving the work of Wie [15] numerically by the present numerical model and compares the numerical and experimental measurements. The model presented in [15] is a stacked microchannel heat sink used for cooling of electronic devices consists of two rows of rectangular microchannels with counter flow configuration. The hydraulic diameter of microchannels is 92 μm and its length is 10 mm. The thermal boundary condition used is constant heat flux of 70 (W/cm^2) subjected on the bottom wall of heat sink, a constant velocity and uniform temperature are applied at the inlet of channels.

The comparison between the numerical results of present model with the numerical and experimental results of [15] is shown in Fig. 3. This figure shows the distribution of experimental and numerical values of wall temperature along the heat sink. From this figure the agreement between the numerical results of [15] and numerical results of the present model are good and maximum error is 1.59% with maximum difference of wall temperature 0.56 K. Also the agreement between the present numerical results and experimental data of [15] is acceptable since the maximum error is 5.1% and maximum difference in wall temperature is 1.7 K. The slight deviation of temperature at the beginning and end of the channel may be due to the end effects and experimental uncertainly.

From these results one can conclude that the built numerical model is reliable and can be used to study the thermal performance of CFMCHEs.

Fig. 4 shows variation of effectiveness with number of channels for fixed volume for three values of Reynolds number $Re = 20, 50$ and 200. From this figure it can be seen that the effectiveness

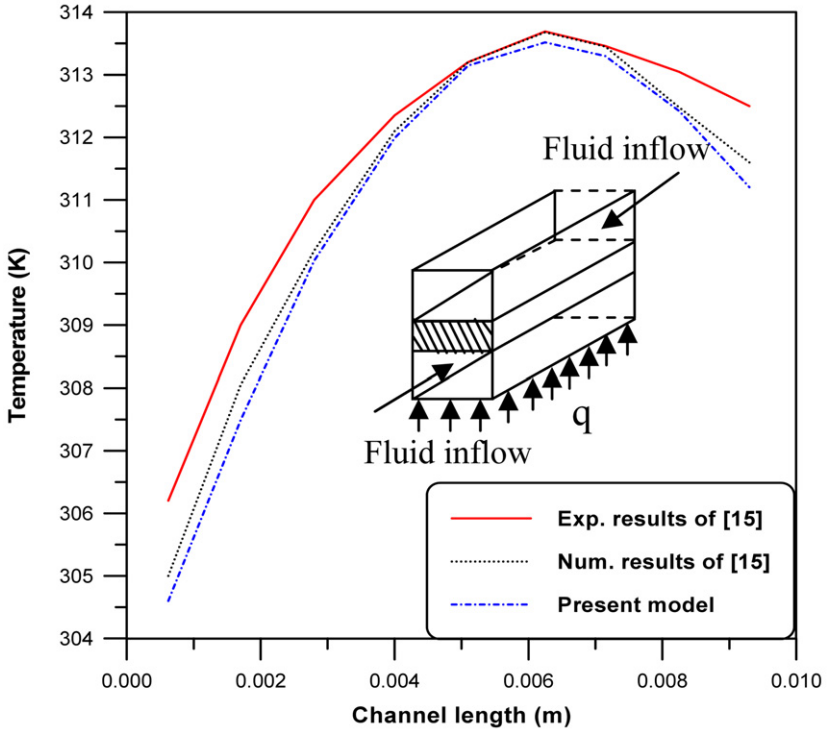

Fig. 3. Comparison of variation of wall temperature along a heat sink ($Re = 66$).

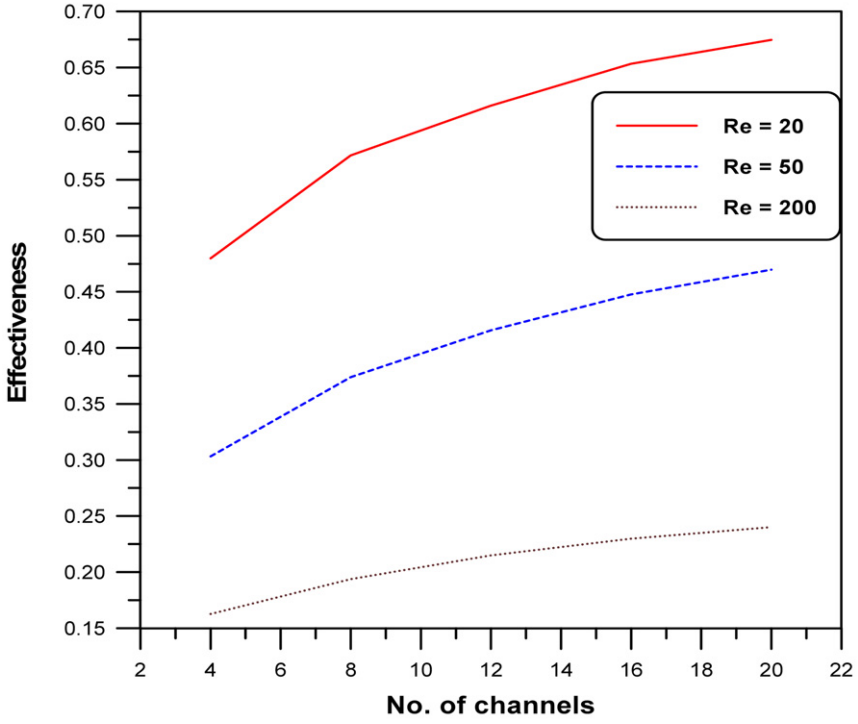

Fig. 4. Variation of effectiveness with number of square channels in a heat exchanger ($Kr = 90$, $Pr = 3.89$).

of CFMCHE increased with increase of number of channels i.e. decrease the volume of channels. This is the main feature of microchannels since it offer higher heat transfer abilities over a small volume and its ability to handle higher heat transfer with decrease of its size. The effectiveness of CFMCHE decreases with increase of Reynolds number due to increase the velocity of flow and therefore decreasing the residence time taken by fluids inside the channels of heat exchanger. Also the increase of effectiveness with increase of channels numbers is higher for low Reynolds numbers. Therefore to obtain higher thermal performance for CFMCHE its better to divide this heat exchanger into large number of channels and work under low flow Reynolds number.

In addition to the advantage of increasing thermal performance with decreasing of channels volume there is a drawback associated with increase of the pressure drop across heat exchanger. Fig. 5 shows variation of total pressure drop in a counter flow

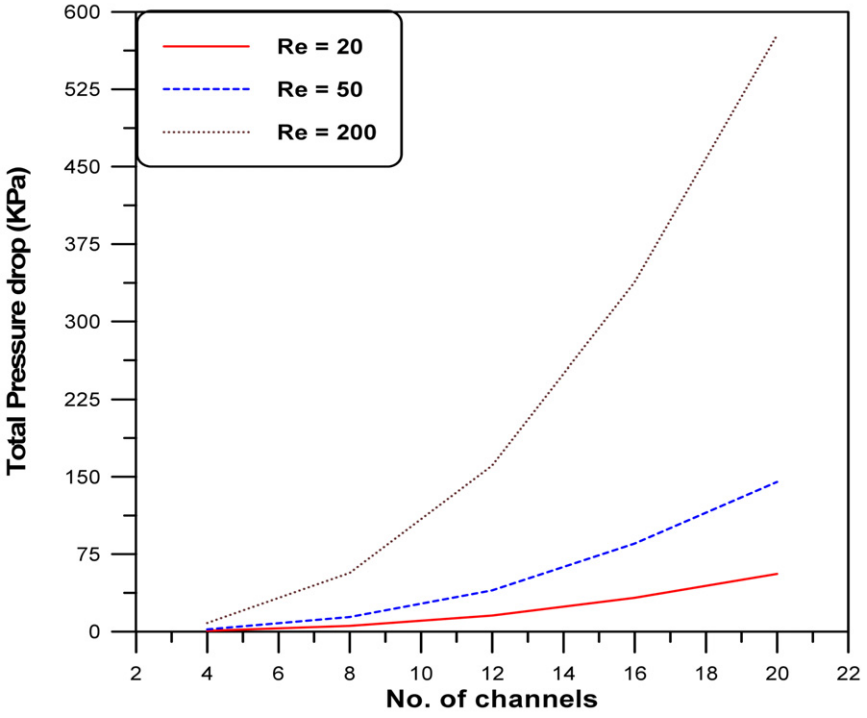

Fig. 5. Variation of total pressure drop in a CFMCHE with number of square channels ($Pr = 3.89$).

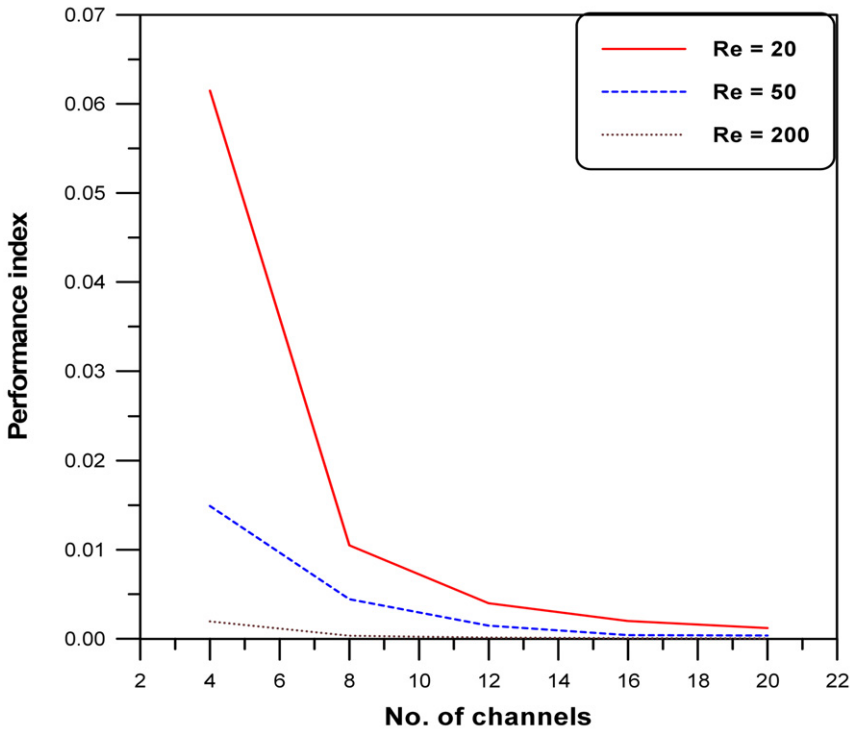

Fig. 6. Variation of performance index with number of square channels ($Kr = 90$).

microchannel heat exchanger with number of channels for three values of Reynolds number $Re = 20, 50$ and 200 and $\Delta P_t = \Delta P_{ch} \times N_{ch}$. Figs. 4–5 illustrate that reducing hydraulic diameter is responsible for large heat transfer performance which lead also to high pressure drop. Therefore increasing or decreasing the channels size in a CFMCHE depends on the application at which this CFMCHE will be used and the penalty of high electrical power. For land based systems such pressure drop may be tolerated therefore the trend is to decrease the size of channels to get high heat transfer benefits. In contrast in space applications the pressure drop across the system must be minimized because incredible payload costs are associated with the total mass of the system (pump, motor, etc.), therefore the size of channels must be increased to avoid the extra increase in pressure drop against the heat transfer characteristics.

Variation of performance index η with number of channels is presented in Fig. 6. From this figure it can be seen that for the same heat exchanger volume, the overall performance is decreased

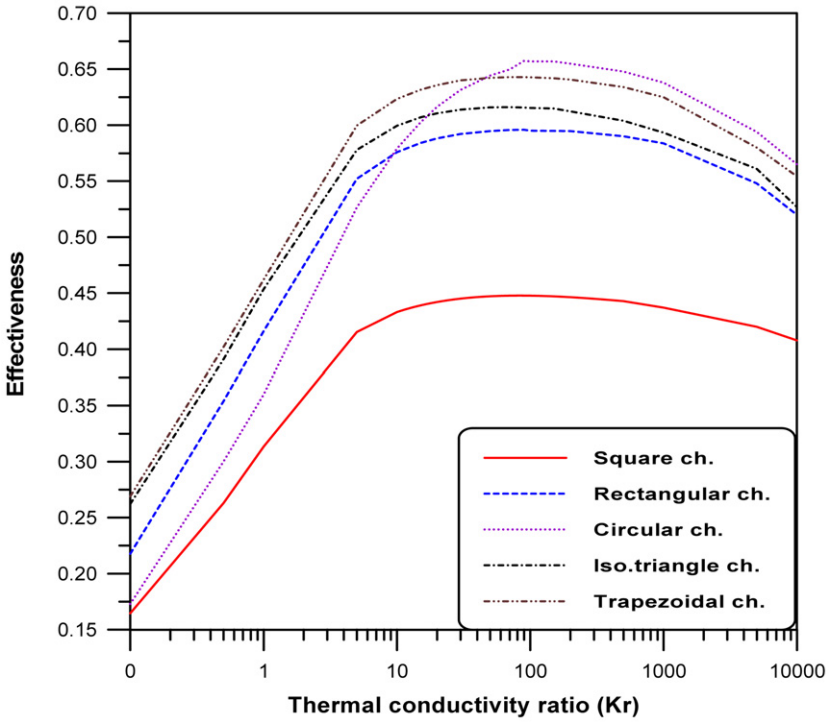

Fig. 7. Variation of thermal effectiveness with *Kr* for different channel shapes ($Re = 50$).

with increasing the number of channels. From heat transfer point of view, it means that a CFMCHE with small channels is the best but from the pressure drop and pumping power point of view the CFMCHE with larger channels are the best. In all cases the flow with low Reynolds number, $Re = 20$ have high performance index, i.e. having higher overall thermal and hydrodynamic performance because it has higher effectiveness and lower pressure drop.

Fig. 7 shows the variation of the effectiveness of the balanced CFMCHE with respect to thermal conductivity ratio (*Kr)* for different channel shapes occupying the same volume of heat exchange unit. From this figure it can be seen that for low values of thermal conductivity ratio the trapezoidal channel is the best followed by iso-triangle but with increasing (*Kr*) the circular channel gives highest effectiveness due to increase the effect of axial conduction which lead to decrease of effectiveness in trapezoidal and triangular shapes more than in circular cross-section. These two shapes have area of separating wall larger than for circular and other shapes. Also it can be seen that for all shapes studied the effectiveness increased with increase of thermal conductivity ratio due to reduction in thermal resistance of the wall until reach the optimal value of *Kr* which gives maximum effectiveness. As *Kr* is further raised beyond the optimal value the effectiveness of the CFMCHE is dropped due to the presence of axial heat conduction.

Distribution of pressure drop along the channel length for various shapes under consideration is shown in Fig. 8. The channel which has largest pressure drop is the triangular since it has lowest hydraulic diameter followed by trapezoidal. The square channel has the lowest pressure drop since it has high hydraulic diameter and maximum cross-sectional area compared with other shapes. Note that channels with different profile have different hydraulic diameter or volume even though they have the same volume for the heat exchange unit.

The two important parameters in a CFMCHE design are effectiveness and pressure drop which are represented as performance index η. Variation of performance index with *Kr* at $Re = 50$ for different channel profiles is illustrated in Fig. 9. The circular channel has the high η since it has largest effectiveness with low values of pressure drop. This means that the circle channel is the best option for a counter flow MCHE. The second best option would be square channels followed by other shapes. Also it can be seen from this figure that the performance index increased with increase *Kr* until reached its maximum value and then decreased due to increase the effect of axial conduction. This trend remained the same in Fig. 10 which represent the variation of η^* with respect to *Kr* at $Re = 50$. It gives an indication about the overall performance of a CFMCHE where the circle is the best shape.

Variation of effectiveness of counter flow MCHE with *Re* for different channel shapes at $Kr = 90$ is illustrated in Fig. 11. This value of *Kr* is the optimized conduction ratio which gives the highest effectiveness as shown in Fig. 7. From Fig. 11, it can be seen that at low values of Reynolds number the channels with circular shape has the highest effectiveness while at high *Re* the CFMCHE with triangular channels become the best followed by trapezoidal and then the circular one. This may be explained due to the effect of entrance region since the entrance length is longer in triangle and trapezoid than the circle channel and other shapes. The effect of entrance region increases with increase in Reynolds numbers. Therefore in applications at high values of Reynolds number, $Re > 200$, the triangular shape is preferred while for low Reynolds number applications, $Re < 200$, the circular shape is preferred. Also in general the effectiveness decreased with increasing *Re* due to increase of flow velocity and there by reducing the residence time inside the CFMCHE.

Fig. 12 shows the variation of performance index with *Re* for different channels shapes at $Kr = 90$. From this figure it can be noticed that the circular channel has the higher performance index than other shapes. Moreover the performance index is decreased with increase of *Re*. This is due to the reduction of effectiveness and increase of the pressure drop.

Fig. 13 shows the variation of η^* with *Re*. The trend is the same as in Fig. 12, hence the circular channel is the best shape as it gives high heat transfer rate with low pumping power.

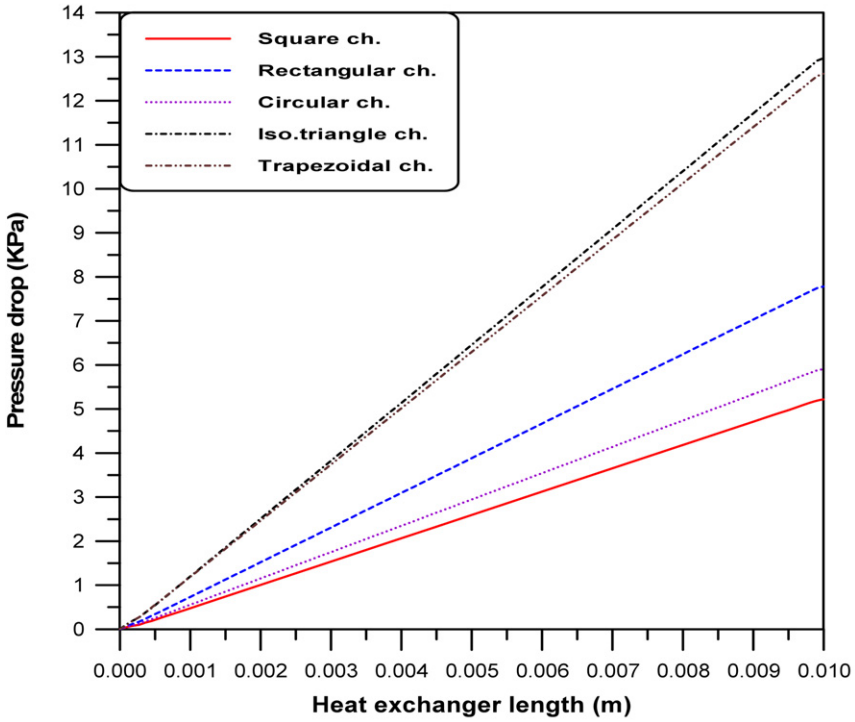

Fig. 8. Variation of pressure drop for one channel of different shapes ($Re = 50$).

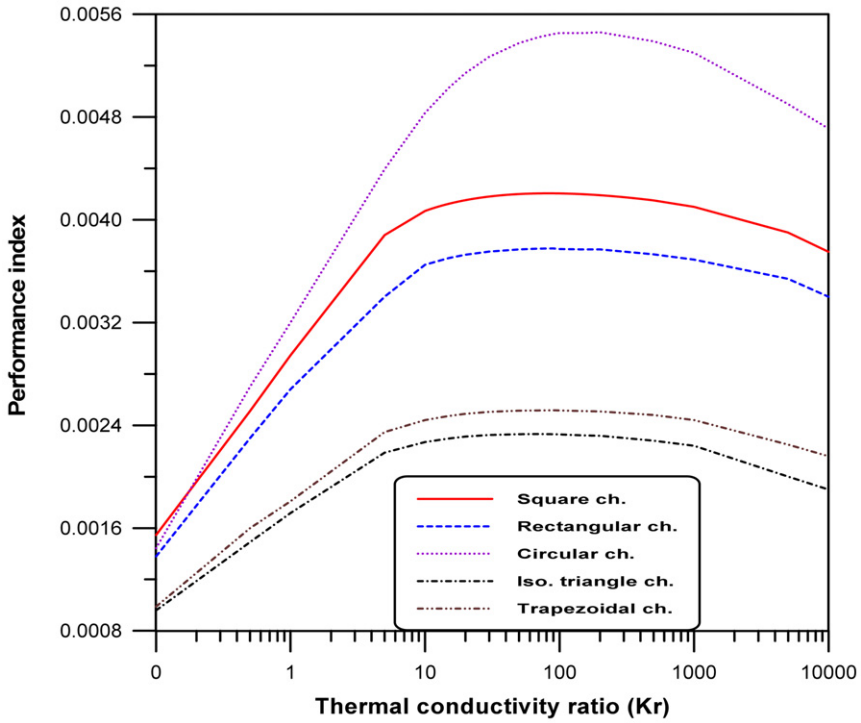

Fig. 9. Variation of performance index η with Kr for different channel shapes ($Re = 50$).

For practical design applications a new correlation is developed to calculate the effectiveness of a balanced counter flow microchannel heat exchanger with square channels as a function of affecting parameters, $\varepsilon = f(Vr, Re, Kr)$.

It should be mentioned that in spite of high performance in microchannel heat exchanger with circle cross section, microchannel heat exchangers with square channels have more applications in related industries. Since square channels have the highest performance after circle channels and lowest pressure drop. Based on the numerical results presented in this paper and by using linear algebra technique with the aid of Matlab package a correlation for heat exchanger effectiveness and performance index are developed for the range of:

$$20 \leqslant Re \leqslant 900 \quad \text{and} \quad 0.024 \leqslant Vr \leqslant 0.20$$

as follows:

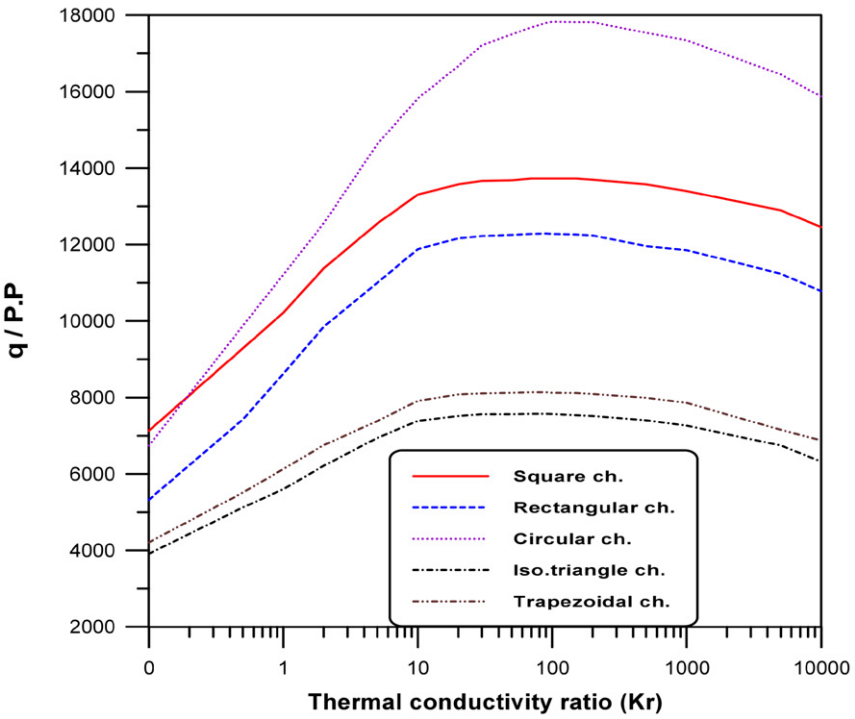

Fig. 10. Variation of heat transfer rate over pumping power required for different channel shapes ($Re = 50$).

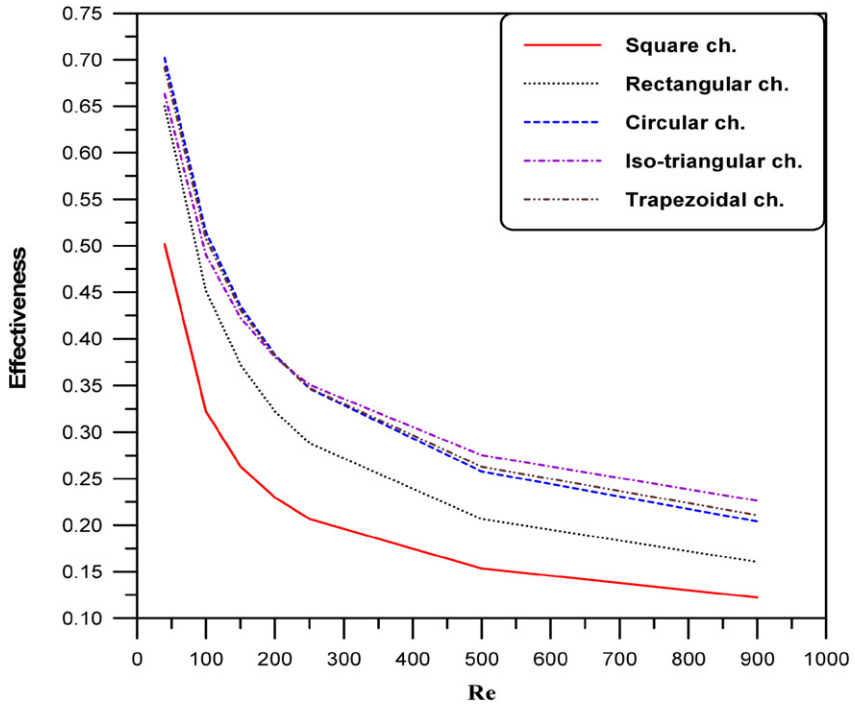

Fig. 11. Effectiveness versus Re for different channel shape ($Kr = 90$).

For $0.1 \leqslant Kr \leqslant 90$

$$\varepsilon = \left(312.7e^{(0.00068\,Kr)} - 297e^{(-0.93\,Kr)}\right) Re^{-0.55}\, Vr^{-0.065} \tag{20}$$

with 15% mean error.

For $91 \leqslant Kr \leqslant 10000$

$$\varepsilon = 164.95\, Re^{-0.44}\, Vr^{-0.148}\, Kr^{-0.025} \tag{21}$$

with 2.8% mean error.

Based on the numerical results for square channels another correlations for the performance index are obtained to get an indication about the overall performance of counter flow microchannel heat exchangers for $20 \leqslant Re \leqslant 900$ and $0.024 \leqslant Vr \leqslant 0.20$ as follows:

For $0.1 \leqslant Kr \leqslant 90$

$$\eta = \left(280.5e^{(0.000745\,Kr)} - 266.5e^{(-0.94\,Kr)}\right) Re^{-1.60}\, Vr^{1.99} \tag{22}$$

with 30% mean error.

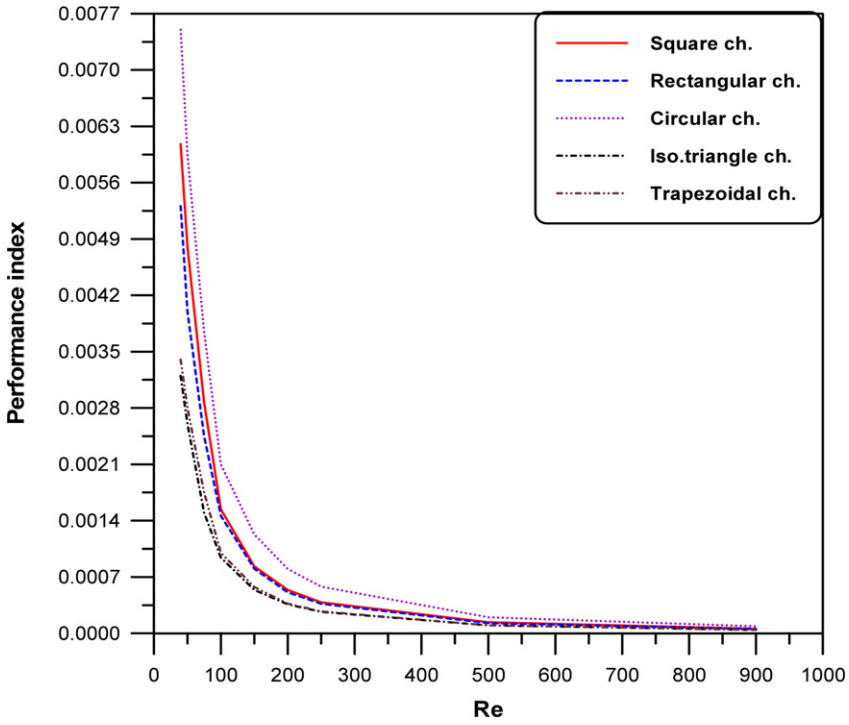

Fig. 12. Performance index versus *Re* for different channel shapes ($Kr = 90$).

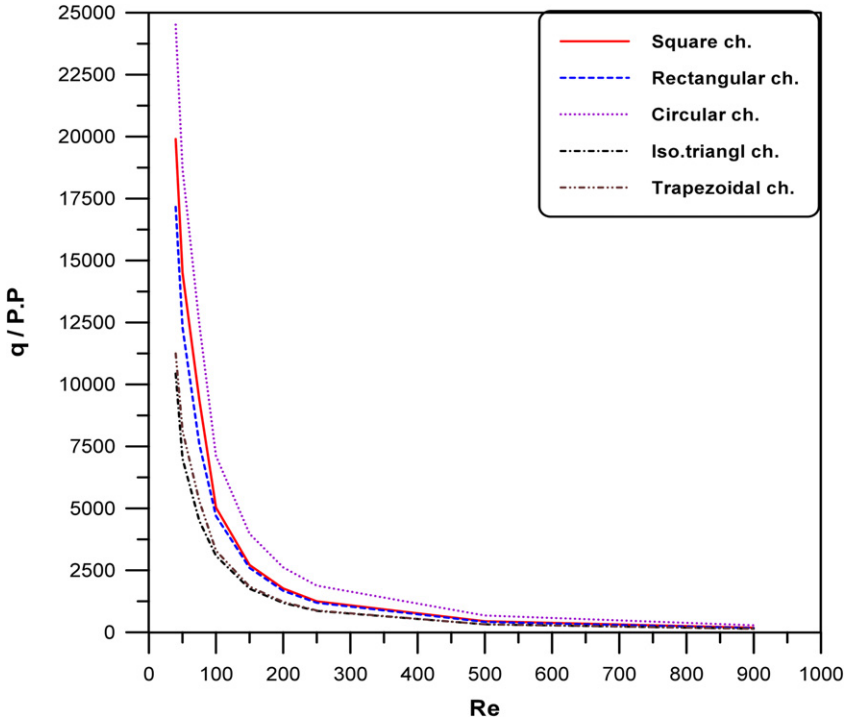

Fig. 13. Heat transfer rate over pumping power versus *Re* for different channel shapes ($Kr = 90$).

For $91 \leqslant Kr \leqslant 10000$

$$\eta = 150.30\, Re^{-1.48}\, Vr^{1.94}\, Kr^{-0.024} \tag{23}$$

with 0.24% mean error.

High mean error in relations (20) and (22) with the compared numerical results is due to sharp variation of η with low value of Kr ($Kr < 90$). But for higher Kr variation is more smooth.

5. Conclusion

In this paper numerical simulation is made to study the effect of size and shape of channels in counter flow microchannel heat exchangers. From the results it is concluded that:

1. By decreasing the volume of each channel or increasing number of channels in a certain CFMCHE, heat transfer increases and required pressure drop and pumping power is also in-

creased. Therefore the decision to increase or decrease the number of channels in a CFMCHE depends on the application.
2. Effect of various channels shape on heat transfer and pressure drop shows that the circular shape gives the best overall performance including both thermal and hydrodynamic. The second best overall performance is provided by square channels.
3. Irrespective of the profile of the channel the performance indices decreased with increase in Reynolds number.
4. Correlations for predicting effectiveness (ε) as well the performance index (η) of a CFMCHE have been developed in this study. These correlations are based on *Re*, *Kr* and *Vr*, and are fairly valid over a wide range of operating parameters.

References

[1] M. Bahrami, M.M. Yovanovich, J.R. Culham, A novel solution for pressure drop in singly connected microchannels of arbitrary cross-section, Int. J. Heat Mass Transfer 50 (2007) 2492–2502.
[2] Z.Y. Guo, Z.X. Li, Size effect on single-phase channel flow and heat transfer at micro scale, Int. J. Heat Fluid Flow 24 (2003) 284–298.
[3] D.B. Tuckerman, R.F. Pease, High performance heat sinking for VLSI, IEEE Electron. Dev. Lett. 2 (1981) 126–129.
[4] X.F. Peng, G.P. Petrson, Convective heat transfer and flow friction for water flow in microchannel structures, Int. J. Heat Mass Transfer 39 (1996) 2599–2608.
[5] D.A. Rachkovskij, E.M. Kussul, S.A. Talayev, Heat exchange in short microtubes and micro heat exchangers with low hydraulic losses, in: Microsystems Technologies, vol. 4, Springer, 1998, pp. 151–158.
[6] H. Albakhit, A. Fakheri, A hybrid approach for full numerical simulation of heat exchangers, in: Proceedings of ASME Heat Transfer Summer Conference, July 17–22, 2005, San Francisco, CA, USA, 2005.
[7] J.J. Brandner, E. Anurjew, L. Buhn, E. Hansjosten, T. Henning, U. Schygulla, A. Wenka, K. Schubert, Concept and realization of microstructure heat exchangers for enhanced heat transfer, Experimental Thermal and Fluid Science 30 (2006) 801–809.
[8] K. Foli, T. Okaba, M. Olhofer, Y. Jon, B. Sendhoff, Optimization of micro heat exchanger: CFD, analytical approach and multi-objective evolutionary algorithms, Int. J. Heat Mass Transfer 49 (2006) 1090–1099.
[9] Tri Lam Ngo, Yasuyoshi Kato, Konstantin Nikitin, Takao Ishizuka, Heat transfer and pressure drop correlations of microchannel heat exchanger with S-shaped and zigzag fins for carbon dioxide cycles, Experimental Thermal and Fluid Science 32 (2007) 560–570.
[10] K.A. Hoffmann, Computational Fluid Dynamics for Engineers, Engineering Educational System, 1993.
[11] M. Farid, M. Smith, R. Sabbah, S. Al-Hallaj, Miniaturized refrigeration system with advanced PCM micro encapsulation technology, in: 5th Conference on Nanochannels, Microchannels, and Minichannels, June 18–20, 2007, Puebla, Mexico.
[12] S.V. Patankar, Numerical Heat Transfer and Fluid Flow, Taylor & Francis, 1980.
[13] C.Y. Zhao, T.J. Lu, Analysis of microchannel heat sinks for electronics cooling, Int. J. Heat Mass Transfer 45 (2002) 4857–4869.
[14] D. Liu, P.S. Lee, Numerical investigation of fluid flow and heat transfer in microchannel heat sinks, in: ME 605 Convection of Heat and Mass, ASME, West Lafayette, USA, 2003.
[15] X. Wei, Stacked microchannel heat sinks for liquid cooling of microelectronics devices, PhD thesis, Academic Faculty, Georgia Institute of Technology, 2004.
[16] F. Yan, Numerical simulations of high Knudsen number gas flow and microchannel electro kinetic liquid flows, PhD thesis, Faculty of Drexel University, USA, 2003.